



Lateral Gene Transfer Drives Metabolic Flexibility in the Anaerobic Methane-Oxidizing Archaeal Family *Methanoperedenaceae*

Andy O. Leu,^a  Simon J. Mcllroy,^{a,b} Jun Ye,^a Donovan H. Parks,^a Victoria J. Orphan,^c Gene W. Tyson^{a,b}

^aAustralian Centre for Ecogenomics, School of Chemistry and Molecular Biosciences, University of Queensland, St. Lucia, Australia

^bCentre for Microbiome Research, School of Biomedical Sciences, Queensland University of Technology (QUT), Translational Research Institute, Woolloongabba, Australia

^cDepartment of Geological and Planetary Sciences, California Institute of Technology, Pasadena, California, USA

Andy O. Leu and Simon J. Mcllroy contributed equally to this work. Author order reflects the order in which the authors joined the project.

ABSTRACT Anaerobic oxidation of methane (AOM) is an important biological process responsible for controlling the flux of methane into the atmosphere. Members of the archaeal family *Methanoperedenaceae* (formerly ANME-2d) have been demonstrated to couple AOM to the reduction of nitrate, iron, and manganese. Here, comparative genomic analysis of 16 *Methanoperedenaceae* metagenome-assembled genomes (MAGs), recovered from diverse environments, revealed novel respiratory strategies acquired through lateral gene transfer (LGT) events from diverse archaea and bacteria. Comprehensive phylogenetic analyses suggests that LGT has allowed members of the *Methanoperedenaceae* to acquire genes for the oxidation of hydrogen and formate and the reduction of arsenate, selenate, and elemental sulfur. Numerous membrane-bound multiheme *c*-type cytochrome complexes also appear to have been laterally acquired, which may be involved in the direct transfer of electrons to metal oxides, humic substances, and syntrophic partners.

IMPORTANCE AOM by microorganisms limits the atmospheric release of the potent greenhouse gas methane and has consequent importance for the global carbon cycle and climate change modeling. While the oxidation of methane coupled to sulfate by consortia of anaerobic methanotrophic (ANME) archaea and bacteria is well documented, several other potential electron acceptors have also been reported to support AOM. In this study, we identify a number of novel respiratory strategies that appear to have been laterally acquired by members of the *Methanoperedenaceae*, as they are absent from related archaea and other ANME lineages. Expanding the known metabolic potential for members of the *Methanoperedenaceae* provides important insight into their ecology and suggests their role in linking methane oxidation to several global biogeochemical cycles.

KEYWORDS ANME, AOM, comparative genomics, methane, *Methanoperedenaceae*

Anaerobic oxidation of methane (AOM) is an important microbiological process moderating the release of methane from anoxic waters and sediments into the atmosphere (1–4). Several diverse uncultured microbial lineages have been demonstrated to facilitate AOM. The bacterium “*Candidatus* Methyloirabilis oxyfera” is proposed to couple AOM to denitrification from nitrite, generating oxygen from nitric oxide for the activation of methane (5). Different lineages of anaerobic methanotrophic (ANME) archaea are hypothesized to mediate AOM through the reversal of the methanogenesis pathway and conserve energy using mechanisms similar to those found in methylotrophic and acetoclastic methanogens (6). Unlike methanogens, most of these ANMEs encode a large repertoire of multiheme *c*-type cytochromes (MHCs), which are

Citation Leu AO, Mcllroy SJ, Ye J, Parks DH, Orphan VJ, Tyson GW. 2020. Lateral gene transfer drives metabolic flexibility in the anaerobic methane-oxidizing archaeal family *Methanoperedenaceae*. *mBio* 11:e01325-20. <https://doi.org/10.1128/mBio.01325-20>.

Editor Mark J. Bailey, CEH, Oxford University

Copyright © 2020 Leu et al. This is an open-access article distributed under the terms of the [Creative Commons Attribution 4.0 International license](https://creativecommons.org/licenses/by/4.0/).

Address correspondence to Gene W. Tyson, gene.tyson@qut.edu.au.

Received 18 May 2020

Accepted 27 May 2020

Published 30 June 2020

proposed to mediate direct interspecies electron transfer to syntrophic sulfate-reducing bacteria (SRB) (7, 8) and/or the reduction of metal oxides and humic acids (9–12).

Currently, several clades within the archaeal phylum *Euryarchaeota* have been shown to be capable of anaerobic methanotrophy and include ANME-1a and -1b, ANME-2a to -2c, *Methanoperedenaceae* (formerly known as ANME-2d), and ANME-3 (13–15). Marine ANME lineages are often observed to form consortia with SRB, with ANME-1 and ANME-2 (a, b, and c) being associated with multiple genera within the *Desulfobacterales* and *Desulfobulbaceae* (13, 16–20), thermophilic ANME-1 being associated with “*Candidatus Desulfofervidus auxilii*” (8, 21), and ANME-3 being associated with SRBs of the *Desulfobulbus* (22). While members of the family *Methanoperedenaceae* have also recently been associated with SRB of the family *Desulfobulbaceae* in a freshwater lake sediment (23), they also appear to oxidize methane independently using a range of electron acceptors. The type species of this family, “*Candidatus Methanoperedens nitroreducens*,” was originally enriched in a bioreactor and shown to couple AOM to the reduction of nitrate via a laterally transferred nitrate reductase (15). Subsequently, “*Candidatus Methanoperedens sp.*” strain BLZ1 was also found to encode a laterally transferred nitrite reductase, which is also present in the genome of “*Ca. Methanoperedens nitroreducens*,” potentially allowing these microorganisms to couple AOM to dissimilatory nitrate reduction to ammonia (DNRA) (24). More recently, three novel species belonging to the *Methanoperedenaceae* were enriched in bioreactors demonstrated to couple AOM to the reduction of insoluble iron or manganese oxides (9, 12). These microorganisms did not encode dissimilatory nitrate reduction pathways but instead were inferred to use multiple unique MHCs during metal-dependent AOM to facilitate the transfer of electrons to the metal oxides (9, 12), consistent with the extracellular electron transfer mechanisms proposed for marine ANME organisms (7, 8). Bioreactor performance and 16S rRNA gene amplicon data have also been used to suggest that members of the *Methanoperedenaceae* are capable of AOM coupled to the reduction of selenate and chromium(VI), although this remains to be confirmed with more direct evidence (25, 26). Notably, members of the *Methanoperedenaceae* have been observed to facilitate AOM coupled to multiple terminal electron acceptors within the same natural sediment (27). Individual members of the family can possess such metabolic flexibility, with a lab-enriched species shown to couple AOM to the reduction of nitrate, iron, and manganese oxides (10). Given the relatively poor genomic representation of the *Methanoperedenaceae* and the lack of detailed physiological studies of its members, it is likely that considerable metabolic diversity for the lineage remains to be discovered.

In this study, comparative analysis was conducted on 16 *Methanoperedenaceae* metagenome-assembled genomes (MAGs) recovered from various environments to investigate the metabolic diversity and versatility of the family and to understand the evolutionary mechanisms responsible for these adaptations. These analyses indicate that members of the *Methanoperedenaceae* have acquired a large number of genes through lateral gene transfer (LGT) that potentially allow AOM to be coupled to a wide range of electron acceptors, suggesting that their role in methane oxidation extends beyond environments with nitrate and metal oxides.

RESULTS AND DISCUSSION

Expanding the genomic representation of the *Methanoperedenaceae*. In order to explore the metabolic diversity within the *Methanoperedenaceae*, comparative genomic analysis was performed on both publicly available and newly acquired MAGs (Table 1). The publicly available genomes include six MAGs recovered from bioreactors where AOM is coupled to the reduction of nitrate (“*Ca. Methanoperedens nitroreducens*”; M.Nitro [15], BLZ2 [28], and IPS-1 [29]), iron (“*Ca. Methanoperedens ferrireducens*”; M.Ferri [9]), and manganese (“*Ca. Methanoperedens manganicus*” and “*Ca. Methanoperedens manganireducens*,” Mn-1 and Mn-2, respectively [12]). Also included are two environmental MAGs recovered from groundwater samples from the Horonobe and Mizunami underground research laboratories in Japan (HGW-1 and MGW-1) (30,

TABLE 1 Characteristics of the metagenome-assembled genomes

Bin ID	Genome size (mbp)	No. of scaffolds	N_{50} (scaffolds; bp)	Strain heterogeneity ^a	Compl. (%) ^a	Cont. (%) ^a	%GC	No. of CDSs ^e	Source environment and associated publication	Accession no. ^b	16S rRNA gene ^c
ASW-1	1.52	271	7,386	0.0	87.5	0.0	47.8	1,946	Arsenic-contaminated groundwater, Bangladesh (104)	SRR1563167, SRR1564103, SRR1573565, SRR1573578, SAMN10961276	N
ASW-2	2.63	157	28,058	25.0	94.4	4.8	48.0	2,944	Arsenic-contaminated groundwater, Bangladesh (104)	SRR1563167, SRR1564103, SRR1573565, SRR1573578, SAMN10961277	N
ASW-3	2.51	100	44,967	0.0	100.0	1.3	50.7	2,892	Arsenic-contaminated groundwater, Bangladesh (104)	SRR1563167, SRR1564103, SRR1573565, SRR1573578, SAMN10961278	N
ASW-4	2.24	155	24,336	0.0	97.1	0.7	43.2	2,464	Arsenic-contaminated groundwater, Bangladesh (104)	SRR1563167, SRR1564103, SRR1573565, SRR1573578, SAMN10961279	N
ASW-5	2.97	221	19,046	0.0	95.0	2.6	48.9	3,353	Arsenic contaminated groundwater, Bangladesh (104)	SRR1563167, SRR1564103, SRR1573565, SRR1573578, SAMN10961280	N
ASW-6	2.19	68	56,691	66.7	99.4	2.0	46.6	2,472	Arsenic-contaminated groundwater, Bangladesh (104)	SRR1563167, SRR1564103, SRR1573565, SRR1573578, SAMN10961281	Y
BLZ1 ^c	3.74	514	17,508	13.33	96.73	6.56	40.2	4,659	AOM-nitrate bioreactor, Netherlands (24)	LKCM00000000.1	Y
BLZ2	3.74	85	74,304	0.0	99.4	4.6	40.3	4,041	AOM-nitrate reactor, Netherlands (28)	GCA_002487355.1	N
CMD-1	1.85	116	27,949	100.0	98.0	0.7	44.9	2,261	Copper mine tailings dam, Brazil (105)	SRR5161805, SRR5161795, SAMN10961282	N
CMD-2	1.45	221	9,704	0.0	88.4	0.0	44.1	1,786	Copper mine tailings dam, Brazil (105)	SRR5161805, SRR5161795, SAMN10961283	N
HGW-1	2.00	128	24,496	33.3	96.4	2.0	43.2	2,288	Groundwater samples, Japan (31)	GCA_002839545.1	Y
IPS-1	3.52	250	27,331	10.0	97.7	5.9	44.1	3,970	AOM-nitrate bioreactor seeded from paddy field soil, Italy (29)	GCA_900196725.1	Y
M.Ferri	2.91	59	88,069	0.0	98.7	1.3	40.8	3,019	AOM-iron bioreactor, Australia (9)	GCA_003104905.1	Y
M.Nitro	3.20	10	54,4976	0.0	99.7	1.3	43.2	3,428	AOM-nitrate bioreactor, Australia (15)	GCA_000685155.1	Y
MGW-1	2.08	161	17,186	0.0	97.4	3.6	44.8	2,488	Groundwater samples, Japan (30)	Not available ^d	N
Mn-1	3.59	68	87,551	0.0	100.0	1.3	40.6	3,737	AOM-manganese bioreactor, Australia (12)	SAMN10872768	N
Mn-2	3.32	116	49,809	0.0	99.4	4.6	42.9	3,684	AOM-manganese bioreactor, Australia (12)	SAMN10872769	N

^aCompleteness (compl.), contamination (cont.), and strain heterogeneity were estimated using CheckM (33).

^bGenome accession numbers. For the MAGs assembled in this study the SRA accession numbers are also given.

^cThe BLZ1 genome was not used in analyses, as it is almost identical to the BLZ2 genome (99.5% ANI) and has inferior completeness and contamination values. The BLZ1 bioreactor was the parent system of the BLZ2 bioreactor.

^dThis genome was provided by Yohey Suzuki and is associated with the study of Ino and colleagues (30).

^eCDSs, coding sequences; N, no; Y, yes.

31). In order to recover additional genomes belonging to the family, GraftM (32) was used to screen public metagenome sequence data sets from the NCBI for *Methanoperedenaceae*-related 16S rRNA and *mcrA* gene sequences. Subsequent assembly and genome binning on data sets found to contain *Methanoperedenaceae*-like sequences led to the recovery of an additional eight MAGs belonging to the family. Six of these were from arsenic-contaminated groundwater samples (ASW-1-6), and a further two were from sediment and groundwater samples from a copper mine tailings dam (CMD-1 and CMD-2). All 16 MAGs are highly complete ($\geq 87.4\%$), with low contamination ($\leq 5.9\%$) based on 228 *Euryarchaeota*-specific marker genes (Table 1) (33). These genomes vary in GC content from 40.2 to 50.7% and range in size from 1.45 to 3.74 Mbp.

A genome tree including 1,199 publicly available archaeal genomes, based on a concatenated set of 122 marker genes (34), confirmed the phylogenetic placement of the 16 MAGs within the *Methanoperedenaceae*. The genome tree supports that these MAGs form a monophyletic clade sister to the GoM-Arc1 genomes (Fig. 1). These genomes likely represent three separate genera within the family, based on their placement within a reference tree, relative evolutionary distance, FastANI distance, and average amino acid identity (AAI [35]; 61.3 to 89.2%) (see Fig. S1 in the supplemental material). All MAGs were classified as members of the genus “*Ca. Methanoperedens*,” except HGW-1 and ASW-3, which appear to represent independent genus-level lineages (Fig. 1). Phylogenetic analysis of the six MAGs containing 16S rRNA genes was consistent with the genome tree (Fig. S2), supporting their classification as members of the *Methanoperedenaceae* family.

Potential electron donors used by the *Methanoperedenaceae*. Metabolic reconstruction of the *Methanoperedenaceae* MAGs showed that all genomes encoded the central methanogenesis pathway, inclusive of the methyl coenzyme M (methyl-CoM) reductase, supporting their potential for the complete oxidation of methane to CO₂ (Fig. 2 and Fig. S3). The annotation of membrane-bound formate dehydrogenases (FdhAB) in four of the *Methanoperedenaceae* MAGs (Mn-2, ASW-4, ASW-1, and MGW-1) (Fig. 3) suggests that some members of the family may also oxidize formate (E_0 [CO₂/HCOO⁻] = -430 mV) (36). As the enzyme is reversible, these species may also potentially produce formate as a supplementary electron sink during AOM, as suggested for Mn-2 (12). Formate was proposed as a putative electron shuttle between ANME-1 organisms and their syntrophic partner SRB, based on the annotation and expression of *fdhAB* in ANME-1, but this has not been supported with physiological studies (37, 38). The putative formate dehydrogenase encoded in the Mn-2 MAG is phylogenetically related to an FdhA found in the genome of *Caldiarchoaeum subterraneum*, while those encoded by ASW-4, ASW-1, and MGW-1 appear to be more similar to FdhA of *Methanocellaceae* archaeon UBA148 (Fig. 3).

The use of hydrogen (H₂; E_0 = -414 mV [39]) as an electron source was previously suggested for MGW-1 and HGW-1, which encode group 1 membrane-bound NiFe hydrogenase complexes, composed of a NiFe catalytic subunit, a FeS electron transfer subunit, and a membrane-bound *b*-type cytochrome (30, 31). These hydrogenases, along with similar group 1 NiFe hydrogenases identified in the ASW-6 and CMD-2 MAGs, form a monophyletic clade with those encoded by the MAG for “*Candidatus Hydrothermarchaeota*” (JdFR-18), which belongs to the archaeal phylum *Hydrothermarchaeota* (40), and several members of the *Halobacterota* (Fig. S4A). The ASW-3 and ASW-5 MAGs encode group 1 NiFe hydrogenases that are basal to Vho/Vht/Vhx hydrogenases encoded by members of the genus *Methanosarcina* (41). As the ASW-5 NiFe hydrogenase does not encode a *b*-type cytochrome (Fig. S4B), it is unclear how electrons are derived from hydrogen. In addition to the membrane-bound NiFe hydrogenases, the M.Nitro MAG was found to carry genes for two different sets of group 3b cytoplasmic hydrogenases (Fig. S4A). The MGW-1 (30) and ASW-2 MAGs also encode group 3b hydrogenases, which have been implicated in hydrogen evolution and NADP (NADPH) reduction (42). Similar complexes have also been shown to have hydrogen oxidation and elemental-sulfur-reducing capabilities (42–44). It is unknown how these

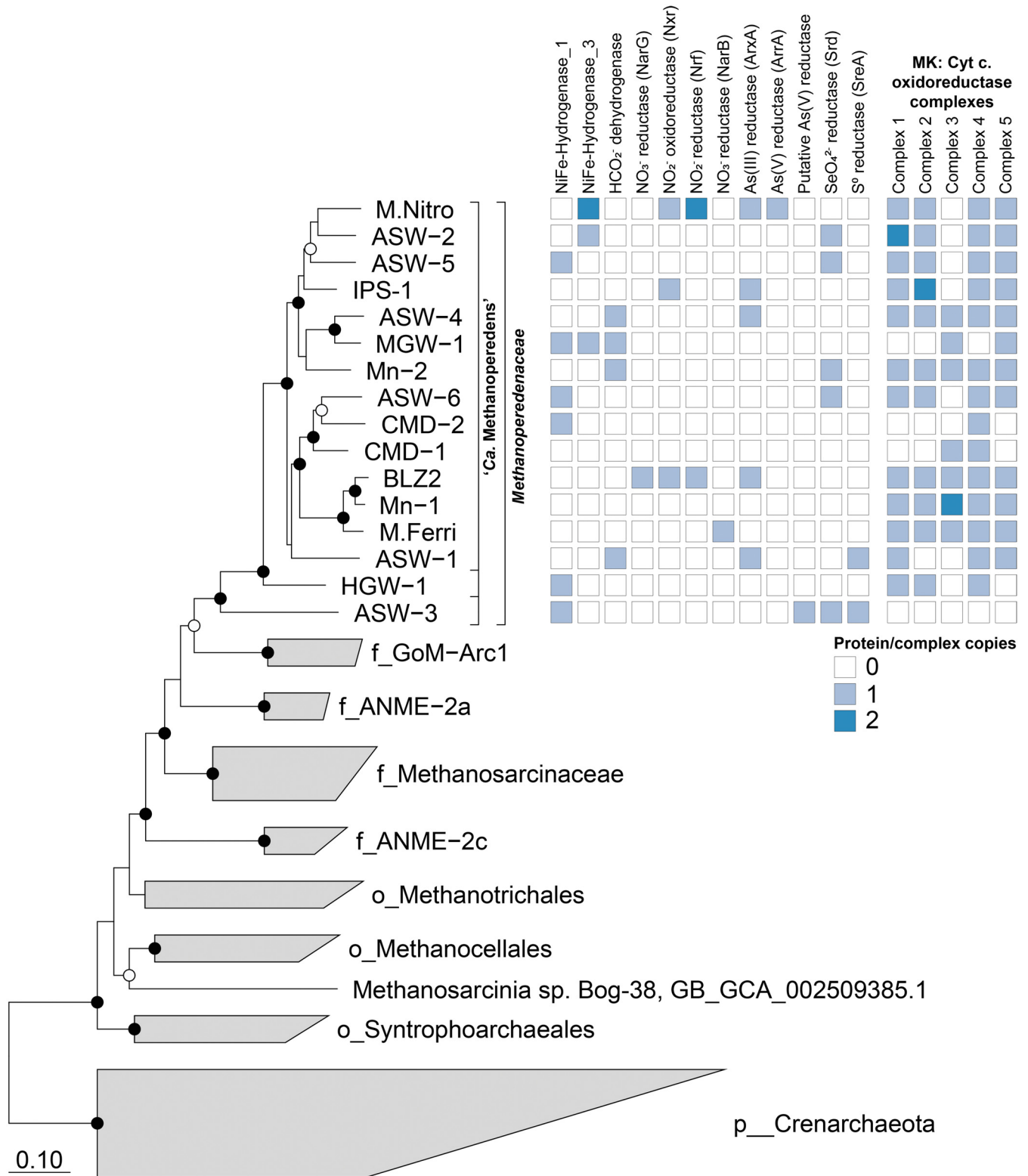


FIG 1 Phylogenetic placement of the *Methanoperedenaceae* MAGs and distribution of potential terminal electron acceptors. The genome tree was inferred using maximum likelihood with a concatenated set of 122 archaeon-specific marker genes. Black and white dots indicate >90% and >70% bootstrap values, respectively. The scale bar represents amino acid nucleotide changes. Based on GTDB-Tk, the family *Methanoperedenaceae* includes three genera, including “*Ca. Methanoperedens*,” which are denoted with brackets. The table to the right of the tree shows the presence/absence of genes associated with potential terminal electron acceptors in each corresponding *Methanoperedenaceae* genome.

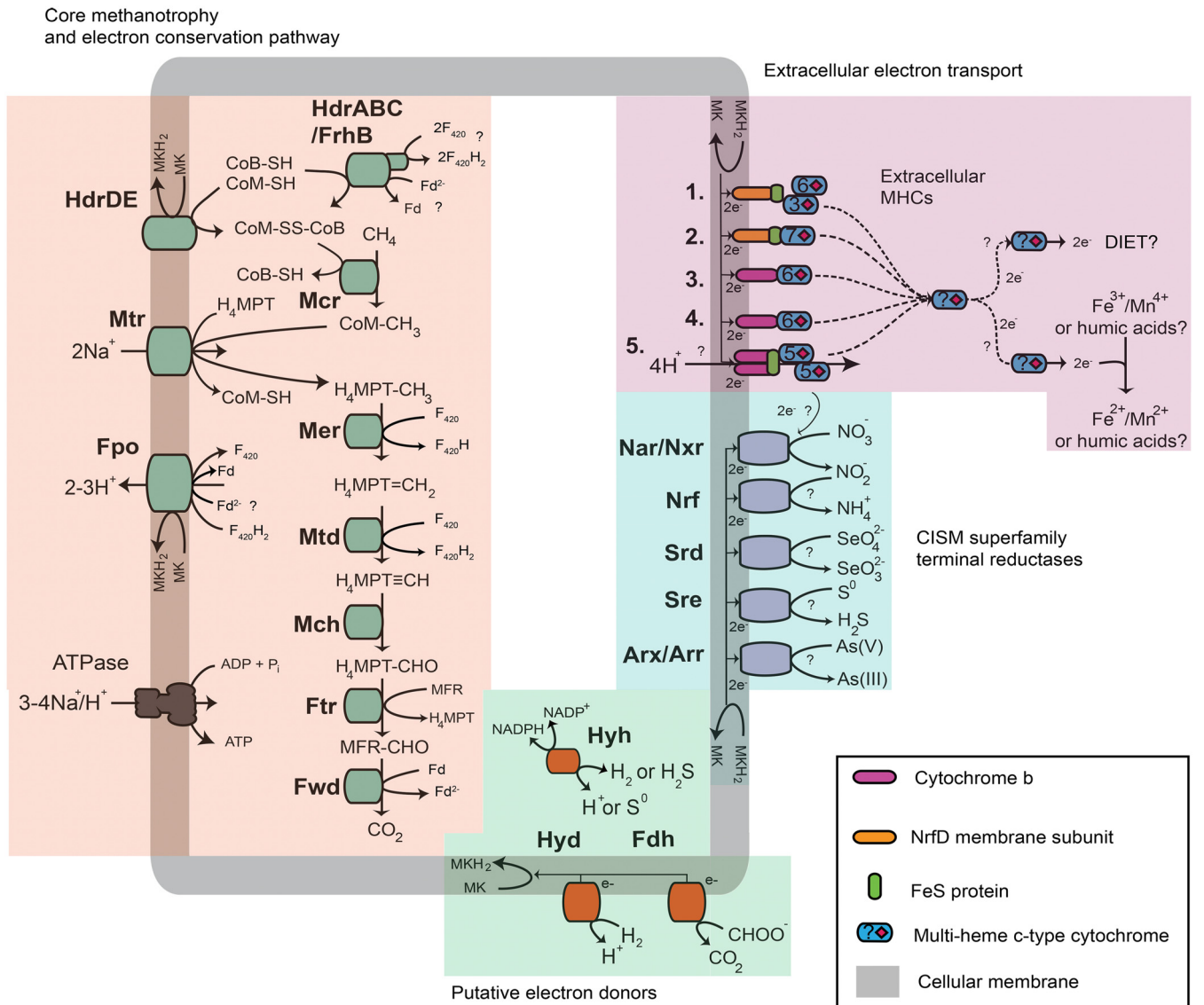


FIG 2 Metabolic capabilities of the *Methanoperedenaceae*. Key metabolic pathways for the anaerobic oxidation of methane, energy conservation mechanisms, hydrogen and formate oxidation, and electron acceptors found within the pangenome of the *Methanoperedenaceae*. Numbers 1 to 5 indicate the different menaquinone:cytochrome c oxidoreductases conserved in the *Methanoperedenaceae* MAGs (Data Set S1A). Abbreviations for enzymes and cofactors in the figure are as follows: H₄MPT, tetrahydromethanopterin; MFR, methanofuran; Fwd, formyl-methanofuran dehydrogenase; Ftr, formylmethanofuran/H₄MPT formyltransferase; Mch, methenyl-H₄MPT cyclohydrolase; Mtd, F₄₂₀-dependent methylene H₄MPT dehydrogenase; Mer, F₄₂₀-dependent methylene-H₄MPT reductase; Mtr, Na⁺-translocating methyl-H₄MPT:coenzyme M (CoM) methyltransferase; Mcr, methyl-CoM reductase; F₄₂₀, F₄₂₀ coenzyme; Fd, ferredoxin; CoM-SH, coenzyme M; CoB-SH, coenzyme B; Hdr, heterodisulfide reductase; Fpo, F₄₂₀H₂ dehydrogenase; Hyd, type 1 NiFe hydrogenase; Hyh, type 3b NiFe hydrogenase; Fdh, formate dehydrogenase; Nar, nitrate reductase; Nrf, nitrite reductase; Srd, selenate reductase; Sre, sulfur reductase; Arx, arsenite oxidase; Arr, arsenate reductase; DIET, direct interspecies electron transfer.

group 3b hydrogenases contribute to energy conservation given their predicted cytoplasmic localization. The functionality of the annotated group 1 and 3 NiFe hydrogenases is supported by the identification of the NiFe binding motifs (L1 and L2) on their NiFe catalytic subunits and the annotation of all or most of the hydrogenase maturation genes (*hypA* to *-F*) on the same *Methanoperedenaceae* MAGs (Data Set S1D). The potential for some *Methanoperedenaceae* to couple the oxidation of hydrogen and/or formate to the reduction of exogenous electron acceptors would be advantageous with the dynamic availability of methane in natural environments (45).

Pathways for energy conservation during AOM in the *Methanoperedenaceae*. All members of the *Methanoperedenaceae* encode the Fpo complex (FpoABCDHIJ₁J₂LMNOF), a homolog of complex I (nuoABCDEFGHIJKLMN), which is

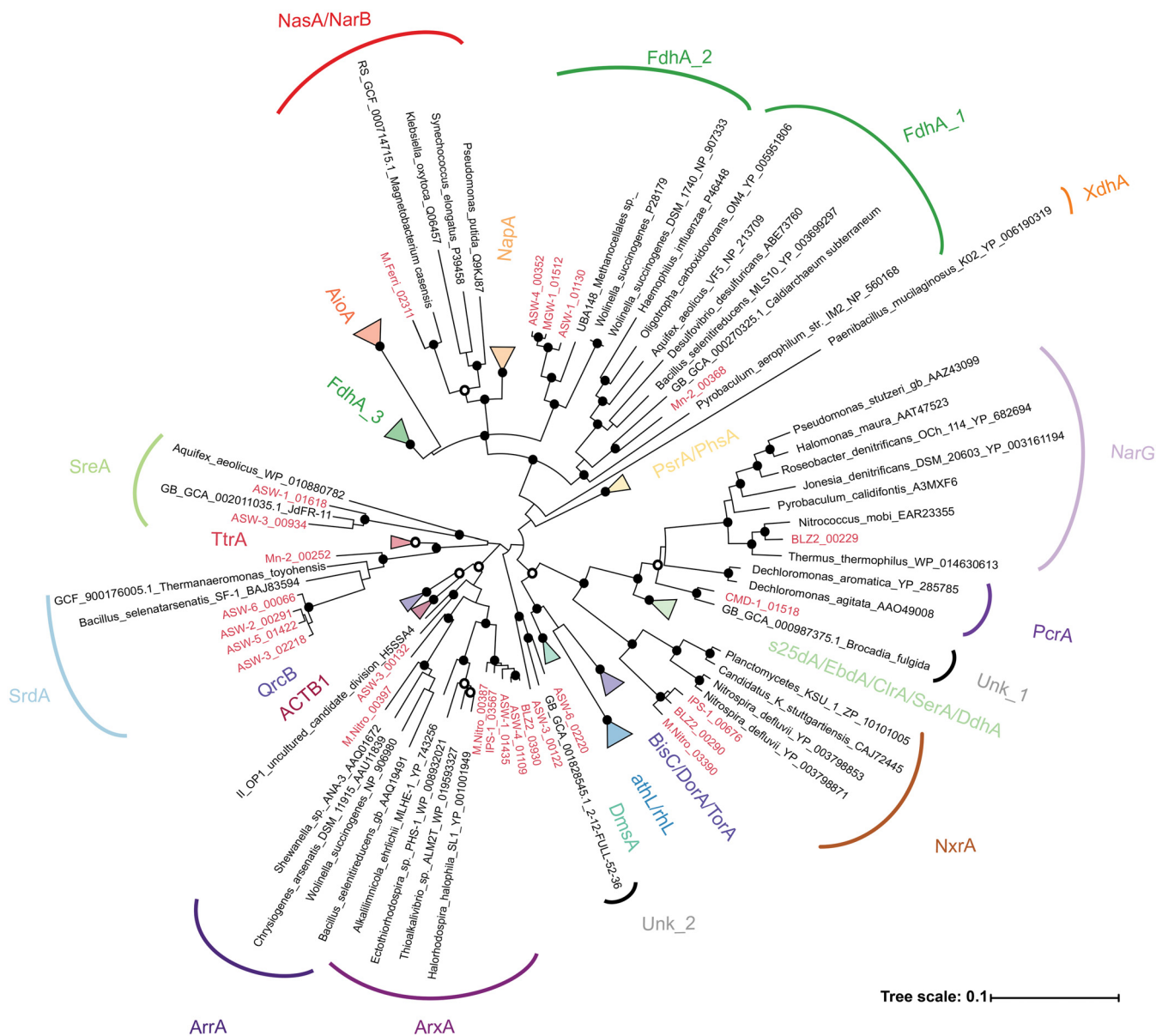


FIG 3 Phylogenetic analysis of the catalytic subunits of the CISM superfamily. Putative genes recovered from the *Methanoperedenaceae* are indicated in red. The gene tree was inferred by maximum likelihood, and support values were calculated via nonparametric bootstrapping. Black and white dots indicate >90% and >70% bootstrap support, respectively. The scale bar represents amino acid changes. ACTB1, alternate complex III, domain of subunit B; ArrA, arsenate reductase; ArxA, arsenite oxidase; AthL, pyrogallol hydroxyltransferase; BisC, biotin sulfoxide reductase; CirA, chlorate reductase; EbdA, ethylbenzene dehydrogenase; s25dA, C25 dehydrogenase; DmsA, DMSO reductase; DorA, DMSO reductase; NapA, nitrate reductase; NarG, nitrate reductase; NasA, assimilatory nitrate reductase; NarB, assimilatory nitrate reductase; NxrA, nitrite oxidoreductase; PsrA, polysulfide reductase; PhsA, thiosulfate reductase; QrcB, quinone reductase complex; TtrA, tetrathionate reductase; DmsA, PcrA, perchlorate reductase; SrdA, Selenate reductase; SreA, sulfur reductase; TorA, trimethylamine *N*-oxide (TMAO) reductase; XdhA, xanthine dehydrogenase; FdhA, formate dehydrogenase; rhL, resorcinol hydroxylase; Unk, unknown putative reductase. Amino acid sequences are included in Data Set S1B.

hypothesized to oxidize $F_{420}H_2$ coupled to the reduction of a membrane-bound soluble electron carrier and translocation of two protons out of the cell (Fig. 2 and Fig. S5A) (41, 46). While members of the *Methanosarcinales* and marine ANME-2a are reported to typically use methanophenazine (MP) as their membrane-bound soluble electron carrier, the *Methanoperedenaceae* and ANME-1 have previously been suggested to use menaquinone (MK) based on the annotation of the fufalosine pathway for MK biosynthesis in several MAGs representing these lineages (47). Comparative genomic analysis of the 16 *Methanoperedenaceae* MAGs revealed that the fufalosine pathway is a conserved feature of all members, except the most basal member, ASW-3 (see below

and Data Set S1A). As has previously been suggested by Arshad et al. (24), the larger difference in redox potential between F_{420} ($E_0 = -360\text{mV}$) and MK ($E_0 = -80\text{mV}$ [48]) than between F_{420} and MP ($E_0 = -165\text{mV}$ [49]) would theoretically allow the Fpo complex to translocate more protons ($3\text{H}^+/2\text{e}^-$) out of the cell for every molecule of F_{420} oxidized, giving a higher overall energetic yield from AOM (Fig. S5B).

Phylogenetic analysis of the Fpo complex in the *Methanoperedenaceae* MAGs showed that the FpoKLMNO subunits are homologous to proteins found in MP-utilizing members of the *Methanosarcinales*. The FpoABCDHIJ₁J₂ subunits are more similar to those found in microorganisms known to use MK and other quinones, which have more positive redox potentials (Fig. S5 and S6; Data Set S1E) (50). As the latter subunits (specifically FpoH) are responsible for the interaction with the membrane-soluble electron carrier pool (51, 52), this observation provides further support to the use of MK by members of the *Methanoperedenaceae*. To our knowledge, this is the first reported example of a lineage encoding a “hybrid” complex I homolog possessing subunits with homology to those found in phylogenetically diverse microorganisms (Fig. S6). The GoM-Arc-I MAGs appear to possess the MK biosynthesis pathway and a hybrid Fpo complex similar to those of the *Methanoperedenaceae* (Fig. S6), suggesting that the evolutionary adaptation of the lineage to utilize MK occurred prior to the divergence of these two related families. Members of the GoM-Arc-1 clade possess Mcr-like complexes (Fig. S3) and are suggested to use short-chain alkanes, possibly ethane (53, 54). Interestingly, the FpoMNO subunits of the ASW-3 MAG cluster with those of the other members of the *Methanoperedenaceae* family, while their FpoABCDHIJ₁J₂KL subunits are most similar to those of the ANME-2a and other members of the *Methanosarcinales* (Fig. S6). While the genes involved in MP biosynthesis are not known, the absence of the MK biosynthesis pathway indicate that ASW-3 likely uses MP. As the most basal lineage of this family, ASW-3 may have adapted to use MP after the evolutionary divergence of the GoM-Arc-I and *Methanoperedenaceae*, although further genomic representation of this lineage is required to verify this hypothesis.

Comparative genomic analyses of the *Methanoperedenaceae* MAGs revealed that none of these genomes encode an Rnf complex, which is hypothesized to reoxidize ferredoxin coupled to the transport of sodium ions out of the cell and the reduction of MP in marine ANME-2a (7, 55) and other methylophilic methanogens (41, 56, 57). In the absence of this complex, ferredoxins may be reoxidized with a “truncated” Fpo complex, similar to the Fpo complex possessed by *Methanosaeta thermophila* (58). Alternatively, an electron-confurcating mechanism may be used for the reoxidation of ferredoxin, coenzyme M, and coenzyme B, coupled to the reduction of two F_{420} molecules via a cytoplasmic complex composed of a heterodisulfide reductase (HdrABC) and a F_{420} hydrogenase subunit B (FrhB) (24). The two additional $F_{420}\text{H}_2$ molecules may subsequently be fed back into the Fpo complex, greatly increasing the overall bioenergetic yield (24) (Fig. 2). All of the *Methanoperedenaceae* MAGs have the genetic potential for these alternate strategies for reoxidation of ferredoxin during AOM; however, further experimental validation is required to test these hypotheses.

Conservation of unique menaquinone: cytochrome c oxidoreductases within the *Methanoperedenaceae*. Five different putative MK:cytochrome c oxidoreductase gene clusters (Fig. 1 and 2; Data Set S1A) that are hypothesized to mediate the transfer of electrons out of the cytoplasmic membrane were identified in the *Methanoperedenaceae* MAGs. These gene clusters include a noncanonical bc1/b6f complex adjacent to two hypothetical proteins and two multiheme (6 hemes) c-type cytochromes (MHCs; group 1), two clusters where a b-type cytochrome is adjacent to a 6-heme MHC (groups 2 and 3), and another two clusters where an NrfD-like transmembrane protein is adjacent to an electron-transferring 4Fe-4S ferredoxin iron-sulfur protein and MHCs (groups 4 and 5) (Fig. 2). These bc and NrfD complexes are frequently found in other metal-reducing microorganisms and mediate electron transport from the cytoplasm to the periplasm (59–61).

Most of the 16 *Methanoperedenaceae* MAGs (except CMD-1 and ASW-3) have more than one of these MK:cytochrome oxidoreductase complexes, and 10 have at least four

(Fig. 1). ASW-3 is the only MAG not to encode any MK:cytochrome *c* oxidoreductases, which is consistent with its putative use of MP. A gene encoding a cytochrome *b* found to be most similar to that of “*Ca. Methanohalarchaeum thermophilum*” was identified in ASW-3; however, in the absence of a collocated MHC gene, the extracellular electron transfer step for this microorganism is unclear.

Phylogenetic analysis of the membrane-bound subunits of the MK:cytochrome *c* oxidoreductases (Fig. 2), which include the NrfD subunits (from groups 1 and 2) and the *b*-type cytochromes (from groups 3, 4, and 5), showed that they have been potentially laterally transferred from diverse donors (Fig. S7). The *Methanoperedenaceae* NrfD subunits formed independent clusters with sequences from members of the *Dehalococcoidales* family RBG-16-60-22 (group 1) and a single MAG (RBG-16-55-9) from the candidate phylum Bipolaricaulota (group 2) (Fig. S7A). The *b*-type cytochromes of the *Methanoperedenaceae* belong to three distinct clades (Fig. S7B). The *b*-type cytochromes from groups 3 and 4 clustered with proteins from GoM-ArcI, indicating vertical genetic inheritance from an ancestor of these two families, and group 5 proteins clustered with those from the class *Archaeoglobi* (40).

The conservation of multiple conserved laterally transferred MK:cytochrome *c* oxidoreductases in most of the *Methanoperedenaceae* MAGs may contribute to the reported ability of members of the family to reduce a variety of electron acceptors with a range of redox potentials that include Fe(III) oxide reduction (–100mV to 100 mV) (62), nitrate (+433 mV) (24), and Mn(IV) (+380 mV) (36). Transcriptomic analyses have shown that different MK:cytochrome *c* oxidoreductases are expressed in different species of the genus “*Ca. Methanoperedens*” during AOM coupled to the reduction of Fe(III) oxides (9), Mn(IV) oxides (12), and nitrate (15, 24). A similar phenomenon has been observed for the species *Geobacter sulfurreducens*, where different extracellular electron pathways were used when different electron acceptors were reduced (63).

Potential electron acceptors used by the *Methanoperedenaceae*. Annotation of the *Methanoperedenaceae* MAGs revealed a wide array of genes associated with previously undescribed respiratory strategies for the family that appear to have been acquired via LGT. Principally, these are putative terminal oxidoreductase complexes belonging to the complex-iron-sulfur-molybdenum (CISM) superfamily that were absent in the genomes of related archaeal lineages (Fig. 3). These complexes are composed of a catalytic subunit, an iron-sulfur protein, and a membrane-bound subunit and facilitate the transfer of electrons between the electron acceptor/donor and the MK pool (Fig. 2).

As previously reported, the MAGs M.Nitro, BLZ2, and IPS-1 encode respiratory nitrate reductases that are part of the CISM superfamily and have been demonstrated to mediate AOM coupled to nitrate reduction (15, 24, 29). Based on phylogenetic analysis (Fig. 3), genes encoding cytoplasmic nitrite oxidoreductases (NxrA) were identified in the IPS-1, BLZ2, and M.Nitro MAGs, and a nitrate reductase closely related to NarG proteins was identified in the BLZ2 MAG. Of the *Methanoperedenaceae* MAGs, only the M.Nitro and BLZ2 MAGs possess a putative nitrite reductase (NrfA) for DNRA. The M.Ferri MAG encodes an assimilatory nitrate reductase (NarB/NasA) most similar to a protein encoded by “*Candidatus Magnetobacterium casensis*” (Fig. 3). However, in the absence of an annotated nitrite reductase in the M.Ferri MAG, the potential of this microorganism for assimilatory nitrate reduction is unclear.

Multiple MAGs (ASW-2,3,5,6 and Mn-2) were also found to encode putative selenate reductases (SrdA) (Fig. 3), suggesting their ability for Se(VI)-dependent AOM. Recently, a bioreactor enrichment of a member of the genus “*Ca. Methanoperedens*” exhibited AOM activity when nitrate was replaced with selenate (26). However, as no meta-omic analyses was conducted for the community, it is unclear if the dominant “*Ca. Methanoperedens*” possessed a putative selenate reductase or if it was directly responsible for the observed selenate reduction.

The ASW-1 and ASW-3 MAGs encode a putative sulfur reductase (SreABC). This annotation is supported by its phylogenetic clustering of the catalytic subunit with SreA

from *Aquifex aeolicus* (Fig. 3), which has been shown to reduce elemental sulfur, as well as tetrathionate and polysulfide (64). This is the first genomic evidence suggesting that members of the *Methanoperedenaceae* may be involved in respiratory sulfur-dependent AOM and warrants further investigation. ANME-1 has been proposed to couple AOM to the reduction of polysulfide in a biogenic hydrocarbon seep sediment, but this was based on the annotation and high expression of a putative sulfide: quinone oxidoreductase (SQR) (65). Genes for dissimilatory sulfate reduction pathways were absent in the *Methanoperedenaceae* MAGs, consistent with other ANME lineages (66). MGW-1 was recently speculated to directly couple AOM to sulfate reduction by utilizing assimilatory sulfate reduction pathways. This hypothesis was based on the lack of large MHCs or identifiable alternate electron acceptor complexes encoded in the MAG (30). Several of the *Methanoperedenaceae* MAGs, and those of other ANME lineages, contain candidate genes associated with assimilatory sulfate reduction, but a dissimilatory role for these has not been shown (66).

The M.Nitro MAG encodes two putative reductases belonging to the arsenate reductase (ArrA) and arsenite oxidase (ArxA) group (Fig. 3). The BLZ2, ASW-1, ASW-4, and IPS-1 MAGs also encode reductases that cluster with the M.Nitro ArxA-like sequence. The ArxA protein has been found to be capable of both arsenite oxidation and arsenate reduction (67), which would allow the *Methanoperedenaceae* possessing these ArxA-like proteins to utilize arsenate as a terminal electron acceptor. Proteins encoded by the ASW-3 and "*Candidatus Acetothermum autotrophicum*" (68) (Fig. 3) form a deep branching clade adjacent to the ArxA and ArrA groups, suggesting that these species might also have the potential to respire on arsenic compounds. It is noteworthy that the ASW-1, -3, and -4 MAGs were recovered from a Bangladesh arsenic-contaminated groundwater sample (Table 1), indicating a role for LGT in their niche-specific adaptation. The possibility of AOM coupled to arsenate [As(V)] reduction has important environmental implications given the wide distribution of arsenic in nature, including subsurface drinking water aquifers (69), and the toxicity and mobility of its reduced form, arsenite [As(III)] (70, 71). Arsenic reduction and mobilization have been linked to an inflow of organic carbon in contaminated aquifers where methane (~1 mM) and arsenate cooccur (72, 73).

Additional putative oxidoreductase clades that are not closely associated with any well-characterized CISM proteins were also found in the *Methanoperedenaceae* MAGs. This includes two proteins encoded by the ASW-3 and ASW-6 MAGs that cluster with a protein of unknown function from a "*Candidatus Brocadiales*" MAG (74) and the CMD-1 protein that clusters with a protein from "*Candidatus Brocadia fulgida*," an ammonium-oxidizing and nitrite-reducing microorganism (75). In general, given the large range of substrates utilized by the CISM superfamily and the few biochemically characterized proteins, the predicted functions of all those annotated in the *Methanoperedenaceae* require empirical verification. Nonetheless, the range of putative CISM superfamily proteins encoded by members of the family likely indicates diverse respiratory strategies that remain to be characterized.

Diversity of the MHCs in the *Methanoperedenaceae*. Members of the *Methanoperedenaceae* possess a diverse repertoire of MHCs which have been suggested to facilitate the transfer of electrons from the reoxidation of MK to metal oxides (9, 10, 76) or direct interspecies electron transfer (DIET) to a syntrophic partner. Analyses of the *Methanoperedenaceae* revealed that they possess between 3 (MGW-1) and 49 (IPS-1) MHCs (containing at least three CXXCH motifs), with an average of 26, the highest average of any archaeal family (Data Sets S1F and S1G). Notably, relatively high numbers of MHCs per genome are almost exclusively found in microorganisms associated with DIET, metal and/or sulfur reduction, such as the *Geobacteraceae* (77) (≤ 87 MHCs), *Shewanellaceae* (78) (≤ 63 MHCs), *Desulfurivibrionaceae* (20), *Desulfuromonadaceae* (20), and *Defferisomataceae* (79) (≤ 50 MHCs) (Data Set S1G). Interestingly, 7 of the 16 members of the *Methanoperedenaceae* encode MHCs with more than 50 heme binding sites (ASW-5, ASW-6, BLZ2, HGW-1, M.ferri, Mn-1, and Mn-2), with the

113-heme MHC encoded by Mn-2 being the largest identified in any microorganism (Data Set S1F).

The 414 putative MHCs identified in the *Methanoperedenaceae* MAGs clustered into 82 orthologous protein families (Fig. S8). Only one protein family (OG0000252) included at least one MHC from each member, which suggests low conservation of these genes within the *Methanoperedenaceae*. Out of the 82 MHC protein families, 14 were identified in at least eight of the 16 MAGs, with five of these found within the conserved MK:cytochrome *c* oxidoreductase clusters. A lack of conservation of MHCs is also observed for anaerobic metal-respiring genus *Geobacter* organisms, where 14% of the MHCs encoded in six analyzed genomes were found to be conserved (60). Thirty-nine of the 82 MHC protein families had significant hits ($1e-20$, $\geq 50\%$ AAI) to homologs from diverse lineages across the bacterial and archaeal domains in the GTDB89 database, indicating potential LGT of these genes (Fig. S9). These lineages notably included the metal-reducing *Geobacteraceae* and *Shewanellaceae*, along with the alkane-oxidizing *Archaeoglobaceae*, *Methylomirabilota* (NC10), and other ANME lineages (Fig. S9).

Putative functions of MHCs in the *Methanoperedenaceae*. Very few of the *Methanoperedenaceae* MHCs could be associated with a specific function. Two orthologous groups were annotated as nitrite: ammonium oxidoreductases (NrfA), with homologs identified in bacterial MAGs classified as *Anaerolineales* (OG0004545; $\geq 66.3\%$ AAI), and the candidate phylum UBP4 (OG0012490, 64.56% AAI). Several MHCs were also identified as part of the MK:cytochrome *c* oxidoreductase clusters, with homologs observed in members of the archaeal family *Archaeoglobaceae* (OG001557, OG000137, OG0001550; $\geq 57.3\%$ AAI) (Fig. S9). MHC/S-layer fusion proteins were suggested to mediate the transfer of electrons across the S-layer for marine ANME-2 (7) and were relatively highly expressed by “*Ca. Methanoperedens manganicus*” and “*Ca. Methanoperedens manganireducens*” during AOM coupled to Mn(IV) reduction (12). Conversely, only low expression of MHC/S-layer protein genes borne by “*Ca. Methanoperedens ferrireducens*” was observed during AOM coupled to Fe(III) reduction (9). In addition, despite all the *Methanoperedenaceae* MAGs containing S-layer proteins, five do not encode MHC proteins with an S-layer domain (ASW-3, CMD-1, CMD-2, HGW-1, and MGW-1), indicating alternative mechanisms for electron transfer across the S-layer to extracellular MHCs for these species.

Predicted extracellular MHCs are hypothesized to facilitate the final transfer of electrons from the *Methanoperedenaceae* to metal oxides (9). Interestingly, “*Ca. Methanoperedens manganicus*” and “*Ca. Methanoperedens manganireducens*” showed differential expression patterns in the complement of shared extracellular MHCs during AOM coupled to Mn(IV) reduction. In addition, no orthologs for the two MHCs highly transcribed by “*Ca. Methanoperedens ferrireducens*” during AOM coupled to Fe(III) reduction (9) were identified in other members of the *Methanoperedenaceae* (OG0011636 and OG0003254) (Fig. S8), suggesting that BLZ2 utilizes a different MHC for iron reduction linked to AOM (10). These observations suggest that the *Methanoperedenaceae* can utilize multiple mechanisms for the reduction of similar metal oxides. Differential expression of conserved MHCs linked to extracellular electron transfer was also observed for different *Geobacteraceae* species enriched on electrodes when they were exposed to the same surface redox potential (80). As suggested for members of the *Geobacteraceae*, the large MHC repertoire possessed by the *Methanoperedenaceae* may enable adaptation to the use of a range of terminal electron acceptors.

This study has substantially improved the genome coverage of the *Methanoperedenaceae*. Comparative genomic analysis of this lineage highlights a metabolic plasticity not found in other ANME clades. The subsequent ability of members of the family to adapt to the use of terminal electron acceptors across a range of redox potentials likely contributes to their success in diverse environments (Table 1). Notably, based on the genome tree (Fig. 1) and the lack of conservation of MHCs (Fig. S8), the acquisition of these genes is not congruent with the genome-based phylogeny of the family,

suggesting niche-specific adaptations as the main driver for these LGT events. While further studies are necessary to verify the general physiology and energy conservation mechanisms of the *Methanoperedenaceae* in different environments, this study provides genomic evidence that members of the family may play key roles in coupling cycling of carbon with selenate, sulfur, and arsenic in addition to nitrate and metal oxides. Continued sequencing and characterization of this lineage will reveal the full extent of their metabolic versatility and influence on global biogeochemical cycles.

MATERIALS AND METHODS

Recovery of the genomes from SRA. The NCBI sequence read archive (SRA [81]) was accessed on the 22nd of March 2017, and 14,516 data sets classified as environmental metagenomes were downloaded. The metagenomic data sets were screened using GraftM (32) to search for 16S rRNA and *mcrA* gene sequences similar to those from members of the *Methanoperedenaceae*. For data sets for which members of the family were detected, all paired-end read sets were trimmed and quality filtered using PEAT v1.2.4 (82). For genomes, CMD-1 and CMD-2 and NCBI accession number [SRR5161805](#) and [SRR5161795](#) reads were coassembled using metaSPAdes version 3.10.0 using the default parameters (83). For the ASW genomes, NCBI accession number [SRR1563167](#), [SRR1564103](#), [SRR1573565](#), and [SRR1573578](#) reads were coassembled using metaSPAdes version 3.10.0, with default parameters (83). Mapping of quality reads was performed using BamM v1.7.3, with default parameters (<https://github.com/ECogenomics/BamM>). Metagenomic assembled genomes were recovered from the assembled metagenomes using uniteM v0.0.14 (<https://github.com/dparks1134/UniteM>). The *Methanoperedenaceae* MAGs were further refined by reassembling the mapped quality trimmed reads with SPAdes using the `-careful` and `-trusted` contig settings. Additional scaffolding and resolving ambiguous bases of the MAGs was performed using the “roundup” mode of FinishM, v0.0.7 (<https://github.com/wwood/finishm>). The completeness and contamination rates of the population bins were assessed using CheckM v1.0.11 (33) with the “lineage_wf” command.

Functional annotation. For all MAGs, open reading frames (ORFs) were called and annotated using Prokka v.1.12 (84). Additional annotation was performed using the blastp “verysensitive” setting in Diamond v0.9.18 (<https://github.com/bbuchfink/diamond.git>) against UniRef100 (accessed September 2017) (85), clusters of orthologous groups (COG) (86), Pfam 31 (87), and TIGRFam (released January 2014) (88). ORFs were also diamond blastp searched against Uniref100 (accessed September 2017) containing proteins with KO identifiers (IDs). The top hit for each gene with an E value of $<1e-3$ was mapped to the KO database (89) using the UniProt ID mapping files. Genes of interest were further verified using the NCBI’s conserved domain search to identify a conserved motif(s) present within the gene (90). Psortb v3.0 (91) was used to predict subcellular localization of the putative proteins. Pred-Tat was used to predict putative signal peptides (92). Putative MHCs were identified by ORFs possessing ≥ 3 CXXCH motifs. Putative MHCs were subsequently searched for cytochrome *c*-type protein domains using hmmersearch (HMMER v.3.1) (93) with PfamA (94).

Construction of genome trees. The archaeal genome tree was constructed using GTDB-Tk (GTDBtk v0.2.2; <https://github.com/ECogenomics/GTDBtk/releases>) with a concatenated set of 122 archaeon-specific conserved marker genes inferred from genomes available in the NCBI database (NCBI RefSeq release 83) (34). Marker genes were identified and aligned in each genome using HMMER v.3.1 (93) and concatenated, and trees were constructed using FastTree v.2.1.8 (95) with the WAG+GAMMA models. Support values were determined using 100 nonparametric bootstrapping with GenomeTreeTK. The trees were visualized using ARB (96) and formatted using Adobe Illustrator (Adobe, USA).

Construction of 16S rRNA gene tree. The 16S rRNA gene was identified in MAGs and used to infer taxonomic assignment of the population genome implementing the SILVA 16S rRNA gene database (version 132). Sequences were aligned with 426 16S rRNA gene sequences retrieved from the SILVA database using SSU-align v0.1 (97). The phylogenetic tree was constructed using FastTree v2.1.8 (95) with the Generalised Time-Reversible and GAMMA models. Support values were determined using 100 nonparametric bootstrapping. The trees were visualized using ARB (96) and formatted using Adobe Illustrator.

Calculation of amino acid identity. The *Methanoperedenaceae* MAGs identified in this study were compared to publicly available genomes of the family. Average amino acid identity (AAI) between the genomes was calculated using orthologous genes identified through reciprocal best BLAST hits using compareM v0.0.5 (<https://github.com/dparks1134/CompareM>).

Identification of orthologous proteins. Homologous proteins across MAGs of all the *Methanoperedenaceae*, GoM-Arc I, ANME-2a, and ANME-2c were identified with OrthoFinder (98) v2.3.3 using default parameters. Gene counts of orthologous groups containing MHCs were used as input for a heatmap using the pheatmap package in R, and hierarchical clustering was performed using ward.D2 (99).

Construction of gene trees. Genes of interest in the *Methanoperedenaceae* MAGs were compared against proteins from the GTDB v83 database (34) using the genetreetk “blast” command to identify closely related sequences. For the generation of the gene tree for catalytic subunits of the CISM superfamily, curated protein sequences were also added in the analysis. Accession numbers and amino acid sequences are included in Data Set S1B. For the generation of the gene tree for the catalytic subunits of the group 1 and group 3 NiFe dehydrogenase, curated sequences from the work of Greening et al. (100) were included in the analysis. Accession numbers and amino acid sequences can be found in Data Set S1C. The sequences were subsequently aligned using mafft v7.221 (101) with the `-auto` function, and

the alignment was trimmed using the trimal v1.2 (<https://github.com/scapella/trimal>) “-automated1” option. A phylogenetic tree was constructed using RAxML v8.2.9 (102) with the following parameters: raxmlHPC-PTHREADS-SSE3 -T 30 -m PROTGAMMALG -p 12345. Bootstrap values were calculated via nonparametric bootstrapping with 100 replicates. The trees were visualized using ARB (96) or iTOL (103) and formatted using Adobe Illustrator (Adobe, USA).

Network analysis of MHCs. Putative MHCs from the GTDB v89 database were identified by ORFs possessing ≥ 3 CXXCH motifs. Putative MHCs were subsequently searched for cytochrome *c*-type protein domains using hmmsearch (HMMER v3.1) (93) with PfamA (94). Proteins from each *Methanoperedenaceae* orthogroup were subjected to a blast search against the GTDB v89 MHC protein database using DIAMOND with an E value cutoff of $1e-20$ and $\geq 50\%$ AAI. The result was visualized in Cytoscape v3.7.1, with clusters that contained only, or no, *Methanoperedenaceae* homologs removed.

Data availability. The genomes assembled in this study have been deposited in the NCBI database under the accession numbers [SAMN10961276](https://doi.org/10.1093/nar/nkz1276) to [SAMN10961283](https://doi.org/10.1093/nar/nkz1283).

SUPPLEMENTAL MATERIAL

Supplemental material is available online only.

FIG S1, PDF file, 0.2 MB.

FIG S2, PDF file, 0.5 MB.

FIG S3, PDF file, 0.1 MB.

FIG S4, PDF file, 0.7 MB.

FIG S5, PDF file, 0.3 MB.

FIG S6, PDF file, 2.1 MB.

FIG S7, PDF file, 0.7 MB.

FIG S8, PDF file, 0.4 MB.

FIG S9, PDF file, 0.5 MB.

DATA SET S1, XLSX file, 0.2 MB.

ACKNOWLEDGMENTS

This work was supported by the Australian Research Council (ARC) (grant FT170100070) and the U.S. Department of Energy’s Office of Biological Environmental Research (grant DE-SC0016469). A.O.L. was supported by an ARC Australian Postgraduate Award, and S.J.M. was partly supported by an ARC Future Fellowship (FT190100211).

We thank the AWMC team, particularly Shihu Hu and Zhiguo Yuan, for their ongoing collaboration working on various “*Ca. Methanoperedens*” enrichments.

We have nothing to disclose.

REFERENCES

- Reeburgh WS. 2007. Oceanic methane biogeochemistry. *Chem Rev* 107:486–513. <https://doi.org/10.1021/cr050362v>.
- Segarra KEA, Schubotz F, Samarkin V, Yoshinaga MY, Hinrichs K-U, Joye SB. 2015. High rates of anaerobic methane oxidation in freshwater wetlands reduce potential atmospheric methane emissions. *Nat Commun* 6:7477. <https://doi.org/10.1038/ncomms8477>.
- Martinez-Cruz K, Sepulveda-Jauregui A, Casper P, Anthony KW, Smemo KA, Thalasso F. 2018. Ubiquitous and significant anaerobic oxidation of methane in freshwater lake sediments. *Water Res* 144:332–340. <https://doi.org/10.1016/j.watres.2018.07.053>.
- Thamdrup B, Steinsdóttir HGR, Bertagnolli AD, Padilla CC, Patin NV, Garcia-Robledo E, Bristow LA, Stewart FJ. 2019. Anaerobic methane oxidation is an important sink for methane in the ocean’s largest oxygen minimum zone. *Limnol Oceanogr* 64:2569–2585. <https://doi.org/10.1002/lno.11235>.
- Ettwig KF, Butler MK, Le Paslier D, Pelletier E, Mangenot S, Kuypers MMM, Schreiber F, Dutilh BE, Zedelius J, de Beer D, Gloerich J, Wessels HJCT, van Alen T, Luesken F, Wu ML, van de Pas-Schoonen KT, Op den Camp HJM, Janssen-Megens EM, Francoijs K-J, Stunnenberg H, Weisenbach J, Jetten MSM, Strous M. 2010. Nitrite-driven anaerobic methane oxidation by oxygenic bacteria. *Nature* 464:543–548. <https://doi.org/10.1038/nature08883>.
- McGlynn SE. 2017. Energy metabolism during anaerobic methane oxidation in ANME archaea. *Microbes Environ* 32:5–13. <https://doi.org/10.1264/jsme2.ME16166>.
- McGlynn SE, Chadwick GL, Kempes CP, Orphan VJ. 2015. Single cell activity reveals direct electron transfer in methanotrophic consortia. *Nature* 526:531–535. <https://doi.org/10.1038/nature15512>.
- Wegener G, Krukenberg V, Riedel D, Tegetmeyer HE, Boetius A. 2015. Intercellular wiring enables electron transfer between methanotrophic archaea and bacteria. *Nature* 526:587–590. <https://doi.org/10.1038/nature15733>.
- Cai C, Leu AO, Xie G-J, Guo J, Feng Y, Zhao J-X, Tyson GW, Yuan Z, Hu S. 2018. A methanotrophic archaeon couples anaerobic oxidation of methane to Fe (III) reduction. *ISME J* 12:1929–1939. <https://doi.org/10.1038/s41396-018-0109-x>.
- Ettwig KF, Zhu B, Speth D, Keltjens JT, Jetten MSM, Kartal B. 2016. Archaea catalyze iron-dependent anaerobic oxidation of methane. *Proc Natl Acad Sci U S A* 113:12792–12796. <https://doi.org/10.1073/pnas.1609534113>.
- Scheller S, Yu H, Chadwick GL, McGlynn SE, Orphan VJ. 2016. Artificial electron acceptors decouple archaeal methane oxidation from sulfate reduction. *Science* 351:703–707. <https://doi.org/10.1126/science.aad7154>.
- Leu AO, Cai C, McIlroy SJ, Southam G, Orphan VJ, Yuan Z, Hu S, Tyson GW. 2020. Anaerobic methane oxidation coupled to manganese reduction by members of the *Methanoperedenaceae*. *ISME J* 14:1030–1041. <https://doi.org/10.1038/s41396-020-0590-x>.
- Knittel K, Lösekann T, Boetius A, Kort R, Amann R. 2005. Diversity and distribution of methanotrophic archaea at cold seeps. *Appl Environ Microbiol* 71:467–479. <https://doi.org/10.1128/AEM.71.1.467-479.2005>.
- Orphan VJ, House CH, Hinrichs K-U, McKeegan KD, DeLong EF. 2002. Multiple archaeal groups mediate methane oxidation in anoxic cold seep sediments. *Proc Natl Acad Sci U S A* 99:7663–7668. <https://doi.org/10.1073/pnas.072210299>.
- Haroon MF, Hu S, Shi Y, Imelfort M, Keller J, Hugenholtz P, Yuan Z, Tyson GW. 2013. Anaerobic oxidation of methane coupled to nitrate

- reduction in a novel archaeal lineage. *Nature* 500:567–570. <https://doi.org/10.1038/nature12375>.
16. Orphan VJ, Hinrichs KU, Ussler W, Paull CK, Taylor LT, Sylva SP, Hayes JM, Delong EF. 2001. Comparative analysis of methane-oxidizing archaea and sulfate-reducing bacteria in anoxic marine sediments. *Appl Environ Microbiol* 67:1922–1934. <https://doi.org/10.1128/AEM.67.4.1922-1934.2001>.
 17. Pernthaler A, Dekas AE, Brown CT, Goffredi SK, Embaye T, Orphan VJ. 2008. Diverse syntrophic partnerships from deep-sea methane vents revealed by direct cell capture and metagenomics. *Proc Natl Acad Sci U S A* 105:7052–7057. <https://doi.org/10.1073/pnas.0711303105>.
 18. Hatzenpichler R, Connon SA, Goudeau D, Malmstrom RR, Woyke T, Orphan VJ. 2016. Visualizing in situ translational activity for identifying and sorting slow-growing archaeal-bacterial consortia. *Proc Natl Acad Sci U S A* 113:E4069–E4078. <https://doi.org/10.1073/pnas.1603757113>.
 19. Schreiber L, Holler T, Knittel K, Meyerdierks A, Amann R. 2010. Identification of the dominant sulfate-reducing bacterial partner of anaerobic methanotrophs of the ANME-2 clade. *Environ Microbiol* 12:2327–2340. <https://doi.org/10.1111/j.1462-2920.2010.02275.x>.
 20. Skennerton CT, Chourey K, Iyer R, Hettich RL, Tyson GW, Orphan VJ. 2017. Methane-fueled syntrophy through extracellular electron transfer: uncovering the genomic traits conserved within diverse bacterial partners of anaerobic methanotrophic archaea. *mBio* 8:e00530–17. <https://doi.org/10.1128/mBio.00530-17>.
 21. Holler T, Widdel F, Knittel K, Amann R, Kellermann MY, Hinrichs K-U, Teske A, Boetius A, Wegener G. 2011. Thermophilic anaerobic oxidation of methane by marine microbial consortia. *ISME J* 5:1946–1956. <https://doi.org/10.1038/ismej.2011.77>.
 22. Niemann H, Lösekann T, de Beer D, Elvert M, Nadalig T, Knittel K, Amann R, Sauter EJ, Schlüter M, Klages M, Foucher JP, Boetius A. 2006. Novel microbial communities of the Haakon Mosby mud volcano and their role as a methane sink. *Nature* 443:854–858. <https://doi.org/10.1038/nature05227>.
 23. Su GY, Zopf J, Yao HY, Steinle L, Niemann H, Lehmann MF. 2019. Manganese/iron-supported sulfate-dependent anaerobic oxidation of methane by archaea in lake sediments. *Limnol Oceanogr* 65:863–875. <https://doi.org/10.1002/lno.11354>.
 24. Arshad A, Speth DR, de Graaf RM, den Camp HJO, Jetten MS, Welte CU. 2015. A metagenomics-based metabolic model of nitrate-dependent anaerobic oxidation of methane by *Methanoperedens*-like archaea. *Front Microbiol* 6:1423. <https://doi.org/10.3389/fmicb.2015.01423>.
 25. Lu Y-Z, Fu L, Ding J, Ding Z-W, Li N, Zeng R. 2016. Cr(VI) reduction coupled with anaerobic oxidation of methane in a laboratory reactor. *Water Res* 102:445–452. <https://doi.org/10.1016/j.watres.2016.06.065>.
 26. Luo J-H, Chen H, Hu S, Cai C, Yuan Z, Guo J. 2018. Microbial selenate reduction driven by a denitrifying anaerobic methane oxidation biofilm. *Environ Sci Technol* 52:4006–4012. <https://doi.org/10.1021/acs.est.7b05046>.
 27. Shen LD, Ouyang L, Zhu YZ, Trimmer M. 2019. Active pathways of anaerobic methane oxidation across contrasting riverbeds. *ISME J* 13:752–766. <https://doi.org/10.1038/s41396-018-0302-y>.
 28. Berger S, Frank J, Martins PD, Jetten MS, Welte CU. 2017. High-quality draft genome sequence of “*Candidatus Methanoperedens* sp.” strain BLZ2, a nitrate-reducing anaerobic methane-oxidizing archaeon enriched in an anoxic bioreactor. *Genome Announc* 5:e01159-17. <https://doi.org/10.1128/genomeA.01159-17>.
 29. Vaksmaa A, Guerrero-Cruz S, van Alen TA, Cremers G, Ettwig KF, Lücke C, Jetten MSM. 2017. Enrichment of anaerobic nitrate-dependent methanotrophic “*Candidatus Methanoperedens nitroreducens*” archaea from an Italian paddy field soil. *Appl Microbiol Biotechnol* 101:7075–7084. <https://doi.org/10.1007/s00253-017-8416-0>.
 30. Ino K, Hersedorf AW, Konno U, Kouduka M, Yanagawa K, Kato S, Sunamura M, Hirota A, Togo YS, Ito K, Fukuda A, Iwatsuki T, Mizuno T, Komatsu DD, Tsunogai U, Ishimura T, Amano Y, Thomas BC, Banfield JF, Suzuki Y. 2018. Ecological and genomic profiling of anaerobic methane-oxidizing archaea in a deep granitic environment. *ISME J* 12:31–47. <https://doi.org/10.1038/ismej.2017.140>.
 31. Hersedorf AW, Amano Y, Miyakawa K, Ise K, Suzuki Y, Anantharaman K, Probst A, Burstein D, Thomas BC, Banfield JF. 2017. Potential for microbial H₂ and metal transformations associated with novel bacteria and archaea in deep terrestrial subsurface sediments. *ISME J* 11:1915–1929. <https://doi.org/10.1038/ismej.2017.39>.
 32. Boyd JA, Woodcroft BJ, Tyson GW. 2018. GraftM: a tool for scalable, phylogenetically informed classification of genes within metagenomes. *Nucleic Acids Res* 46:e59. <https://doi.org/10.1093/nar/gky174>.
 33. Parks DH, Imelfort M, Skennerton CT, Hugenholtz P, Tyson GW. 2015. CheckM: assessing the quality of microbial genomes recovered from isolates, single cells, and metagenomes. *Genome Res* 25:1043–1055. <https://doi.org/10.1101/gr.186072.114>.
 34. Parks DH, Chuvochina M, Waite DW, Rinke C, Skarshewski A, Chaumeil P-A, Hugenholtz P. 2018. A standardized bacterial taxonomy based on genome phylogeny substantially revises the tree of life. *Nat Biotechnol* 36:996–1004. <https://doi.org/10.1038/nbt.4229>.
 35. Konstantinidis KT, Tiedje JM. 2005. Towards a genome-based taxonomy for prokaryotes. *J Bacteriol* 187:6258–6264. <https://doi.org/10.1128/JB.187.18.6258-6264.2005>.
 36. Thauer RK, Jungermann K, Decker K. 1977. Energy conservation in chemotrophic anaerobic bacteria. *Bacteriol Rev* 41:100–180. <https://doi.org/10.1128/MMBR.41.1.100-180.1977>.
 37. Nauhaus K, Treude T, Boetius A, Kruger M. 2005. Environmental regulation of the anaerobic oxidation of methane: a comparison of ANME-I and ANME-II communities. *Environ Microbiol* 7:98–106. <https://doi.org/10.1111/j.1462-2920.2004.00669.x>.
 38. Meyerdierks A, Kube M, Kostadinov I, Teeling H, Glöckner FO, Reinhardt R, Amann R. 2010. Metagenome and mRNA expression analyses of anaerobic methanotrophic archaea of the ANME-1 group. *Environ Microbiol* 12:422–439. <https://doi.org/10.1111/j.1462-2920.2009.02083.x>.
 39. Loach PA. 1976. Oxidation-reduction potentials, absorbance bands and molar absorbance of compounds used in biochemical studies. *Handb Biochem Mol Biol* 1:122–130.
 40. Jungbluth SP, Amend JP, Rappé MS. 2017. Metagenome sequencing and 98 microbial genomes from Juan de Fuca Ridge flank subsurface fluids. *Sci Data* 4:170037. <https://doi.org/10.1038/sdata.2017.37>.
 41. Welte C, Deppenmeier U. 2014. Bioenergetics and anaerobic respiratory chains of acetivlastic methanogens. *Biochim Biophys Acta* 1837:1130–1147. <https://doi.org/10.1016/j.bbabi.2013.12.002>.
 42. Kanai T, Matsuoka R, Beppu H, Nakajima A, Okada Y, Atomi H, Imanaka T. 2011. Distinct physiological roles of the three [NiFe]-hydrogenase orthologs in the hyperthermophilic archaeon *Thermococcus kodakarensis*. *J Bacteriol* 193:3109–3116. <https://doi.org/10.1128/JB.01072-10>.
 43. Ma K, Schicho RN, Kelly RM, Adams M. 1993. Hydrogenase of the hyperthermophile *Pyrococcus furiosus* is an elemental sulfur reductase or sulfhydrogenase: evidence for a sulfur-reducing hydrogenase ancestor. *Proc Natl Acad Sci U S A* 90:5341–5344. <https://doi.org/10.1073/pnas.90.11.5341>.
 44. Berney M, Greening C, Hards K, Collins D, Cook GM. 2014. Three different [NiFe] hydrogenases confer metabolic flexibility in the obligate aerobic *Mycobacterium smegmatis*. *Environ Microbiol* 16:318–330. <https://doi.org/10.1111/1462-2920.12320>.
 45. Stanley EH, Casson NJ, Christel ST, Crawford JT, Loken LC, Oliver SK. 2016. The ecology of methane in streams and rivers: patterns, controls, and global significance. *Ecol Monogr* 86:146–171. <https://doi.org/10.1890/15-1027>.
 46. Deppenmeier U, Blaut M, Mahlmann A, Gottschalk G. 1990. Reduced coenzyme F420: heterodisulfide oxidoreductase, a proton-translocating redox system in methanogenic bacteria. *Proc Natl Acad Sci U S A* 87:9449–9453. <https://doi.org/10.1073/pnas.87.23.9449>.
 47. Timmers PH, Welte CU, Koehorst JJ, Plugge CM, Jetten MS, Stams AJ. 2017. Reverse methanogenesis and respiration in methanotrophic archaea. *Archaea* 2017:1654237. <https://doi.org/10.1155/2017/1654237>.
 48. Tran QH, Uden G. 1998. Changes in the proton potential and the cellular energetics of *Escherichia coli* during growth by aerobic and anaerobic respiration or by fermentation. *Eur J Biochem* 251:538–543. <https://doi.org/10.1046/j.1432-1327.1998.2510538.x>.
 49. Tietze M, Beuchle A, Lamla I, Orth N, Dehler M, Greiner G, Beifuss U. 2003. Redox potentials of methanophenazine and CoB-S-S-CoM, factors involved in electron transport in methanogenic archaea. *Chembiochem* 4:333–335. <https://doi.org/10.1002/cbic.200390053>.
 50. Gonzalez O, Gronau S, Pfeiffer F, Mendoza E, Zimmer R, Oesterheld D. 2009. Systems analysis of bioenergetics and growth of the extreme halophile *Halobacterium salinarum*. *PLoS Comput Biol* 5:e1000332. <https://doi.org/10.1371/journal.pcbi.1000332>.
 51. Jones AJ, Blaza JN, Varghese F, Hirst J. 2017. Respiratory complex I in *Bos taurus* and *Paracoccus denitrificans* pumps four protons across the membrane for every NADH oxidized. *J Biol Chem* 292:4987–4995. <https://doi.org/10.1074/jbc.M116.771899>.
 52. Sazanov LA. 2015. A giant molecular proton pump: structure and mechanism of respiratory complex I. *Nat Rev Mol Cell Biol* 16:375–388. <https://doi.org/10.1038/nrm3997>.

53. Dombrowski N, Seitz KW, Teske AP, Baker BJ. 2017. Genomic insights into potential interdependencies in microbial hydrocarbon and nutrient cycling in hydrothermal sediments. *Microbiome* 5:106. <https://doi.org/10.1186/s40168-017-0322-2>.
54. Borrel G, Adam PS, McKay LJ, Chen L-X, Sierra-García IN, Sieber CMK, Letourneur Q, Ghoulane A, Andersen GL, Li W-J, Hallam SJ, Muyzer G, de Oliveira VM, Inskeep WP, Banfield JF, Gribaldo S. 2019. Wide diversity of methane and short-chain alkane metabolisms in uncultured archaea. *Nat Microbiol* 4:603–613. <https://doi.org/10.1038/s41564-019-0363-3>.
55. Wang F-P, Zhang Y, Chen Y, He Y, Qi J, Hinrichs K-U, Zhang X-X, Xiao X, Boon N. 2014. Methanotrophic archaea possessing diverging methane-oxidizing and electron-transporting pathways. *ISME J* 8:1069–1078. <https://doi.org/10.1038/ismej.2013.212>.
56. Schlegel K, Müller V. 2013. Evolution of Na and H bioenergetics in methanogenic archaea. *Biochem Soc Trans* 41:421–426. <https://doi.org/10.1042/BST20120294>.
57. Schlegel K, Welte C, Deppenmeier U, Müller V. 2012. Electron transport during acetate-clastic methanogenesis by *Methanosarcina acetivorans* involves a sodium-translocating Rnf complex. *FEBS J* 279:4444–4452. <https://doi.org/10.1111/febs.12031>.
58. Welte C, Deppenmeier U. 2011. Membrane-bound electron transport in *Methanosaeta thermophila*. *J Bacteriol* 193:2868–2870. <https://doi.org/10.1128/JB.00162-11>.
59. Anderson I, Risso C, Holmes D, Lucas S, Copeland A, Lapidus A, Cheng J-F, Bruce D, Goodwin L, Pitluck S, Saunders E, Brettin T, Dettler JC, Han C, Tapia R, Larimer F, Land M, Hauser L, Woyke T, Lovley D, Kyrpides N, Ivanova N. 2011. Complete genome sequence of *Ferroglobus placidus* AED112DO. *Stand Genomic Sci* 5:50–60. <https://doi.org/10.4056/signs.2225018>.
60. Butler JE, Young ND, Lovley DR. 2010. Evolution of electron transfer out of the cell: comparative genomics of six *Geobacter* genomes. *BMC Genomics* 11:40. <https://doi.org/10.1186/1471-2164-11-40>.
61. Mardanov AV, Slododkina GB, Slobodkin AI, Beletsky AV, Gavrilov SN, Kublanov IV, Bonch-Osmolovskaya EA, Skryabin KG, Ravin NV. 2015. The *Geoglobus acetivorans* genome: Fe (III) reduction, acetate utilization, autotrophic growth, and degradation of aromatic compounds in a hyperthermophilic archaeon. *Appl Environ Microbiol* 81:1003–1012. <https://doi.org/10.1128/AEM.02705-14>.
62. Straub KL, Schink B. 2004. Ferrihydrite reduction by *Geobacter* species is stimulated by secondary bacteria. *Arch Microbiol* 182:175–181. <https://doi.org/10.1007/s00203-004-0686-0>.
63. Levar CE, Hoffman CL, Dunshee AJ, Toner BM, Bond DR. 2017. Redox potential as a master variable controlling pathways of metal reduction by *Geobacter sulfurreducens*. *ISME J* 11:741–752. <https://doi.org/10.1038/ismej.2016.146>.
64. Guiral M, Tron P, Aubert C, Gloter A, Iobbi-Nivol C, Giudici-Ortoni M-T. 2005. A membrane-bound multienzyme, hydrogen-oxidizing, and sulfur-reducing complex from the hyperthermophilic bacterium *Aquifex aeolicus*. *J Biol Chem* 280:42004–42015. <https://doi.org/10.1074/jbc.M508034200>.
65. Vigneron A, Alsop EB, Cruaud P, Philibert G, King B, Baksmaty L, Lavalée D, Lomans BP, Eloe-Fadrosh E, Kyrpides NC, Head IM, Tesmetzki N. 2019. Contrasting pathways for anaerobic methane oxidation in Gulf of Mexico cold seep sediments. *mSystems* 4:e00091-18. <https://doi.org/10.1128/mSystems.00091-18>.
66. Yu H, Susanti D, McGlynn SE, Skennerton CT, Chourey K, Iyer R, Scheller S, Tavormina PL, Hettich RL, Mukhopadhyay B, Orphan VJ. 2018. Comparative genomics and proteomic analysis of assimilatory sulfate reduction pathways in anaerobic methanotrophic archaea. *Front Microbiol* 9:2917. <https://doi.org/10.3389/fmicb.2018.02917>.
67. Zargar K, Conrad A, Bernick DL, Lowe TM, Stolc V, Hoelt S, Oremland RS, Stolz J, Saltikov CW. 2012. ArxA, a new clade of arsenite oxidase within the DMSO reductase family of molybdenum oxidoreductases. *Environ Microbiol* 14:1635–1645. <https://doi.org/10.1111/j.1462-2920.2012.02722.x>.
68. Takami H, Noguchi H, Takai Y, Uchiyama I, Toyoda A, Nishi S, Chee G-J, Arai W, Nunoura T, Itoh T, Hattori M, Takai K. 2012. A deeply branching thermophilic bacterium with an ancient acetyl-CoA pathway dominates a subsurface ecosystem. *PLoS One* 7:e30559. <https://doi.org/10.1371/journal.pone.0030559>.
69. Nordstrom DK. 2002. Worldwide occurrences of arsenic in ground water. *Science* 296:2143–2145. <https://doi.org/10.1126/science.1072375>.
70. Smedley PL, Kinniburgh D. 2002. A review of the source, behaviour and distribution of arsenic in natural waters. *Appl Geochem* 17:517–568. [https://doi.org/10.1016/S0883-2927\(02\)00018-5](https://doi.org/10.1016/S0883-2927(02)00018-5).
71. Council NR. 1999. Arsenic in drinking water. National Academies Press, Washington, DC.
72. Harvey CF, Swartz CH, Badruzzaman ABM, Keon-Blute N, Yu W, Ali MA, Jay J, Beckie R, Niedan V, Brabander D, Oates PM, Ashfaq KN, Islam S, Hemond HF, Ahmed MF. 2002. Arsenic mobility and groundwater extraction in Bangladesh. *Science* 298:1602–1606. <https://doi.org/10.1126/science.1076978>.
73. Polizzotto ML, Harvey CF, Sutton SR, Fendorf S. 2005. Processes conducive to the release and transport of arsenic into aquifers of Bangladesh. *Proc Natl Acad Sci U S A* 102:18819–18823. <https://doi.org/10.1073/pnas.0509539103>.
74. Anantharaman K, Brown CT, Hug LA, Sharon I, Castelle CJ, Probst AJ, Thomas BC, Singh A, Wilkins MJ, Karaoz U, Brodie EL, Williams KH, Hubbard SS, Banfield JF. 2016. Thousands of microbial genomes shed light on interconnected biogeochemical processes in an aquifer system. *Nat Commun* 7:13219. <https://doi.org/10.1038/ncomms13219>.
75. Gori F, Tringe SG, Kartal B, Marchiori E, Machiori E, Jetten MSM. 2011. The metagenomic basis of anammox metabolism in *Candidatus Brocadia fulgida*. *Biochem Soc Trans* 39:1799–1804. <https://doi.org/10.1042/BST20110707>.
76. Kletzin A, Heimerl T, Flechler J, van Niftrik L, Rachel R, Klingl A. 2015. Cytochromes c in Archaea: distribution, maturation, cell architecture, and the special case of *Ignicoccus hospitalis*. *Front Microbiol* 6:439. <https://doi.org/10.3389/fmicb.2015.00439>.
77. Methé BA, Nelson KE, Eisen JA, Paulsen IT, Nelson W, Heidelberg JF, Wu D, Wu M, Ward N, Beanan MJ, Dodson RJ, Madupu R, Brinkac LM, Daugherty SC, DeBoy RT, Durkin AS, Gwinn M, Kolonay JF, Sullivan SA, Haft DH, Selengut J, Davidsen TM, Zafar N, White O, Tran B, Romero C, Forberger HA, Weidman J, Khouri H, Feldblyum TV, Utterback TR, Van Aken SE, Lovley DR, Fraser CM. 2003. Genome of *Geobacter sulfurreducens*: metal reduction in subsurface environments. *Science* 302:1967–1969. <https://doi.org/10.1126/science.1088727>.
78. Heidelberg JF, Paulsen IT, Nelson KE, Gaidos EJ, Nelson WC, Read TD, Eisen JA, Seshadri R, Ward N, Methe B, Clayton RA, Meyer T, Tsapin A, Scott J, Beanan M, Brinkac L, Daugherty S, DeBoy RT, Dodson RJ, Durkin AS, Haft DH, Kolonay JF, Madupu R, Peterson JD, Umayam LA, White O, Wolf AM, Vamathevan J, Weidman J, Impriali M, Lee K, Berry K, Lee C, Mueller J, Khouri H, Gill J, Utterback TR, McDonald LA, Feldblyum TV, Smith HO, Venter JC, Nealon KH, Fraser CM. 2002. Genome sequence of the dissimilatory metal ion-reducing bacterium *Shewanella oneidensis*. *Nat Biotechnol* 20:1118–1123. <https://doi.org/10.1038/nbt.749>.
79. Slobodkina GB, Reysenbach A-L, Panteleeva AN, Kostrikin NA, Wagner ID, Bonch-Osmolovskaya EA, Slobodkin AI. 2012. *Deferriusoma camini* gen. nov., sp. nov., a moderately thermophilic, dissimilatory iron (III)-reducing bacterium from a deep-sea hydrothermal vent that forms a distinct phylogenetic branch in the Deltaproteobacteria. *Int J Syst Evol Microbiol* 62:2463–2468. <https://doi.org/10.1099/ijs.0.038372-0>.
80. Ishii S, Suzuki S, Tenney A, Nealon KH, Bretschger O. 2018. Comparative metatranscriptomics reveals extracellular electron transfer pathways conferring microbial adaptivity to surface redox potential changes. *ISME J* 12:2844–2863. <https://doi.org/10.1038/s41396-018-0238-2>.
81. Cochrane G, Karsch-Mizrachi I, Takagi T, International Nucleotide Sequence Database Collaboration. 2016. The International Nucleotide Sequence Database Collaboration. *Nucleic Acids Res* 44:D48–D50. <https://doi.org/10.1093/nar/gkv1323>.
82. Li Y-L, Weng J-C, Hsiao C-C, Chou M-T, Tseng C-W, Hung J-H, editors. 2015. PEAT: an intelligent and efficient paired-end sequencing adapter trimming algorithm. *BMC Bioinformatics* 16:S2. <https://doi.org/10.1186/1471-2105-16-S1-S2>.
83. Nurk S, Meleshko D, Korobeynikov A, Pevzner PA. 2017. metaSPAdes: a new versatile metagenomic assembler. *Genome Res* 27:824–116. <https://doi.org/10.1101/gr.213959.116>.
84. Seemann T. 2014. Prokka: rapid prokaryotic genome annotation. *Bioinformatics* 30:2068–2069. <https://doi.org/10.1093/bioinformatics/btu153>.
85. Suzek BE, Huang H, McGarvey P, Mazumder R, Wu CH. 2007. UniRef: comprehensive and non-redundant UniProt reference clusters. *Bioinformatics* 23:1282–1288. <https://doi.org/10.1093/bioinformatics/btm098>.
86. Tatusov RL, Fedorova ND, Jackson JD, Jacobs AR, Kiryutin B, Koonin EV, Krylov DM, Mazumder R, Mekhedov SL, Nikolskaya AN, Rao BS, Smirnov S, Sverdlov AV, Vasudevan S, Wolf YI, Yin JJ, Natale DA. 2003. The COG database: an updated version includes eukaryotes. *BMC Bioinformatics* 4:41. <https://doi.org/10.1186/1471-2105-4-41>.
87. Finn RD, Coghill P, Eberhardt RY, Eddy SR, Mistry J, Mitchell AL, Potter SC, Punta M, Qureshi M, Sangrador-Vegas A, Salazar GA, Tate J, Bate-

- man A. 2016. The Pfam protein families database: towards a more sustainable future. *Nucleic Acids Res* 44:D279–D85. <https://doi.org/10.1093/nar/gkv1344>.
88. Haft DH, Selengut JD, Richter RA, Harkins D, Basu MK, Beck E. 2013. TIGRFAMs and genome properties in 2013. *Nucleic Acids Res* 41: D387–D95. <https://doi.org/10.1093/nar/gks1234>.
 89. Kanehisa M, Sato Y, Kawashima M, Furumichi M, Tanabe M. 2016. KEGG as a reference resource for gene and protein annotation. *Nucleic Acids Res* 44:D457–D462. <https://doi.org/10.1093/nar/gkv1070>.
 90. Marchler-Bauer A, Bryant SH. 2004. CD-Search: protein domain annotations on the fly. *Nucleic Acids Res* 32(Suppl 2):W327–W331. <https://doi.org/10.1093/nar/gkh454>.
 91. Yu NY, Wagner JR, Laird MR, Melli G, Rey S, Lo R, Dao P, Sahinalp SC, Ester M, Foster LJ, Brinkman FSL. 2010. PSORTb 3.0: improved protein subcellular localization prediction with refined localization subcategories and predictive capabilities for all prokaryotes. *Bioinformatics* 26: 1608–1615. <https://doi.org/10.1093/bioinformatics/btq249>.
 92. Bagos PG, Nikolaou EP, Liakopoulos TD, Tsigirios KD. 2010. Combined prediction of Tat and Sec signal peptides with hidden Markov models. *Bioinformatics* 26:2811–2817. <https://doi.org/10.1093/bioinformatics/btq530>.
 93. Eddy SR. 2011. Accelerated profile HMM searches. *PLoS Comput Biol* 7:e1002195. <https://doi.org/10.1371/journal.pcbi.1002195>.
 94. Bateman A, Coin L, Durbin R, Finn RD, Hollich V, Griffiths-Jones S, Khanna A, Marshall M, Moxon S, Sonnhammer EL, Studholme DJ, Yeats C, Eddy SR. 2004. The Pfam protein families database. *Nucleic Acids Res* 32(Suppl 1):D138–D141. <https://doi.org/10.1093/nar/gkh121>.
 95. Price MN, Dehal PS, Arkin AP. 2010. FastTree 2—approximately maximum-likelihood trees for large alignments. *PLoS One* 5:e9490. <https://doi.org/10.1371/journal.pone.0009490>.
 96. Ludwig W, Strunk O, Westram R, Richter L, Meier H, Buchner A. 2004. ARB: a software environment for sequence data. *Nucleic Acids Res* 32:1363–1371. <https://doi.org/10.1093/nar/gkh293>.
 97. Nawrocki EP, Kolbe DL, Eddy SR. 2009. Infernal 1.0: inference of RNA alignments. *Bioinformatics* 25:1335–1337. <https://doi.org/10.1093/bioinformatics/btp157>.
 98. Emms DM, Kelly S. 2015. OrthoFinder: solving fundamental biases in whole genome comparisons dramatically improves orthogroup inference accuracy. *Genome Biol* 16:157. <https://doi.org/10.1186/s13059-015-0721-2>.
 99. Kolde R. 2019. Package ‘pheatmap.’ R Package. <https://cran.r-project.org/web/packages/pheatmap/>.
 100. Greening C, Biswas A, Carere CR, Jackson CJ, Taylor MC, Stott MB, Cook GM, Morales SE. 2016. Genomic and metagenomic surveys of hydrogenase distribution indicate H₂ is a widely utilised energy source for microbial growth and survival. *ISME J* 10:761–777. <https://doi.org/10.1038/ismej.2015.153>.
 101. Katoh K, Standley DM. 2013. MAFFT multiple sequence alignment software version 7: improvements in performance and usability. *Mol Biol Evol* 30:772–780. <https://doi.org/10.1093/molbev/mst010>.
 102. Stamatakis A. 2014. RAxML version 8: a tool for phylogenetic analysis and post-analysis of large phylogenies. *Bioinformatics* 30:1312–1313. <https://doi.org/10.1093/bioinformatics/btu033>.
 103. Letunic I, Bork P. 2016. Interactive tree of life (iTOL) v3: an online tool for the display and annotation of phylogenetic and other trees. *Nucleic Acids Res* 44:W242–W245. <https://doi.org/10.1093/nar/gkw290>.
 104. Layton AC, Chauhan A, Williams DE, Mailloux B, Knappett PS, Ferguson AS, McKay LD, Alam MJ, Matin Ahmed K, van Geen A, Saylor GS. 2014. Metagenomes of microbial communities in arsenic- and pathogen-contaminated well and surface water from Bangladesh. *Genome Announc* 2:e01170-14. <https://doi.org/10.1128/genomeA.01170-14>.
 105. Medeiros JD, Leite LR, Pylro VS, Oliveira FS, Almeida VM, Fernandes GR, Salim ACM, Araujo FMG, Volpini AC, Oliveira G, Cuadros-Orellana S. 2017. Single-cell sequencing unveils the lifestyle and CRISPR-based population history of *Hydrothalea* sp. in acid mine drainage. *Mol Ecol* 26:5541–5551. <https://doi.org/10.1111/mec.14294>.